The influence of the lattice geometry on the thermodynamical properties of two-dimensional spin systems

1998 J. Phys.: Condens. Matter 10 5187

(http://iopscience.iop.org/0953-8984/10/23/019)

J. Phys.: Condens. Matter **10** (1998) 5187–5196. Printed in the UK PII: S0953-8984(98)90469-6

The influence of the lattice geometry on the thermodynamical properties of two-dimensional spin systems

B Mombelli†, O Kahn†, J Leandri‡, Y Leroyer‡, S Meshkov‡ and Y Meurdesoif‡

† Laboratoire des Sciences Moléculaires, Institut de Chimie de la Matière Condensée de Bordeaux, UPR CNRS 9048, Avenue Albert Schweitzer, 33608 Pessac, France

‡ Centre de Physique Théorique et de Modélisation de Bordeaux, Université Bordeaux I, URA CNRS 1537, 19 rue du Solarium, 33174 Gradignan, France

Received 7 January 1998, in final form 25 February 1998

Abstract. Various types of mixed-spin two-dimensional Heisenberg network are investigated by means of Monte Carlo simulations. This study aims at interpreting quantitatively the thermodynamical properties of two-dimensional molecule-based magnets that have been recently synthesized. The proposed model requires that: (i) one of the two magnetic centres has a spin large enough to be treated as a classical spin; (ii) the zero-field Hamiltonian is isotropic; (iii) the quantum spins have only classical spins as neighbours. The quantum Hamiltonian is then replaced by a classical one with effective ferromagnetic interactions. The temperature dependence of both the specific heat and the magnetic susceptibility are calculated. The effects of the lattice geometry are analysed. We obtain for the specific heat a typical curve which is independent of these effects.

1. Introduction

A rather large number of molecule-based magnets have been synthesized and investigated in the last few years [1, 2]. They correspond to low-dimensional magnetic systems, either quasi-one-dimensional [3–8] or, more recently, quasi-two-dimensional ones [9, 10]. The one-dimensional compounds are well modelled as equally spaced magnetic chains, alternating chains involving a unique kind of spin carrier, and two kinds of interaction pathway: mixed-spin chains, ladder-type double chains, etc.

This paper is devoted to two-dimensional Heisenberg mixed-spin compounds in which one of the spins is large enough to be treated as a classical spin and the other is normally treated as a quantum spin. This work is motivated by the synthesis of novel two-dimensional magnetic materials. So far, two types of two-dimensional magnetic lattice have been described. Both have honeycomb-like structure. The former type is obtained using oxalate as the bridging ligand. Mn^{2+} ions in octahedral surroundings are located at the corners of the hexagons, and Cu^{2+} ions in elongated tetragonal surroundings are located at the mid-points of the edges. A strong antiferromagnetic interaction is propagated between the Mn^{2+} and Cu^{2+} ions through the oxalate bridge, so the intralayer interaction is very large as compared to the interlayer interaction. In these compounds the layers are negatively charged, and the nature and magnitude of the interlayer interaction is governed by the size of the counter-cations situated between the layers. In the case of the NBu^{4+} counter-cation,

0953-8984/98/235187+10$19.50

a long-range magnetic transition was observed at 15 K, probably due to the synergy between a very weak magnetic anisotropy and a ferromagnetic interlayer interaction [11]. It has been shown in a previous paper [12] that our model leads to an excellent interpretation of the magnetic properties of this material. The parameters found were as follows: $J = 47.6$ K, $g_{Mn} = 2.0$, and $g_{Cu} = 2.2$. These values are very close to those obtained for both $Cu^{2+}Mn^{2+}$ pairs [3] and chains [7] involving the same bridge. The value of the interaction parameter essentially depends on the nature of the bridging network, and is not very sensitive to the spin geometry.

The latter type of lattice is realized in a series of two-dimensional oxalate-bridged bimetallic compounds which have just been synthesized [10]. In such compounds, the two kinds of magnetic ion alternate at the corners of the hexagons. The layers which are again negatively charged are separated by counter-cations. The general formula of these compounds is $(NBu_4)[M^{II}Ru^{III}(ox)_3]$ where M^{II} is either Mn^{II} ($S = 5/2$) or Fe^{II} ($S = 2$) or Cu^{II} ($S = 1/2$), and the spin carried by the high-field Ru^{3+} ion is $S(Ru) = 1/2$. The interaction is ferromagnetic for Mn and antiferromagnetic for Cu and Fe. In the latter case a ferromagnetic transition occurs at $T_c = 13$ K. We note that other compounds with the same structure have been reported [13–16]. The nature of the spin carriers, however, is not such as to allow one to use the classical–quantum spin approach.

The aim of this paper is to study the influence of the geometry of the spin lattice on the thermodynamical properties of such systems. In this way, we derive from the mixed quantum–classical Heisenberg model a purely classical one with an effective interaction which depends on the lattice geometry. This model is analysed by means of Monte Carlo (MC) simulations. We investigate the different realizations of the hexagonal lattice described above, but also two configurations based on the square lattice.

The paper is organized as follows: the model is developed in the first section, then the Monte Carlo analysis is presented, and the results are discussed in the last section.

2. The model

Let us write down the Heisenberg spin Hamiltonian as

$$\mathcal{H} = J \sum_{\langle ij \rangle} \boldsymbol{S}_i^{(Q)} \cdot \boldsymbol{S}_j^{(C)} - g_1 \mu_B H \sum_{j=1}^{N_C} S_j^{z(C)} - g_2 \mu_B H \sum_{i=1}^{N_Q} S_i^{z(Q)}.$$

Here $\boldsymbol{S}_j^{(C)}$ is the large-spin operator (5/2 for Mn, 2 for Fe) which will be approximated by a classical vector, $S\boldsymbol{s}$, where $\boldsymbol{s}$ is a unit vector and

$$S = \sqrt{S^{(C)}(S^{(C)} + 1)}.$$

The $\frac{1}{2}$-spin quantum operator (for Cu or Ru) is denoted by $S_i^{(Q)} = \frac{1}{2}\boldsymbol{\sigma}_i$ with $\boldsymbol{\sigma}_i$ the Pauli matrices. The interaction parameter J is positive for an antiferromagnetic interaction (in the following, we only consider this case); H is a weak magnetic field applied along the z-direction. $\langle ij \rangle$ stands for a pair of nearest-neighbour spins, N_C is the number of classical spins, and N_Q is the number of quantum spins.

Two kinds of magnetic lattice are investigated, the hexagonal one, which has been realized experimentally, and the square one. For each lattice, the spins can be arranged in two fashions: either the classical spins are attached at each vertex, and the quantum spins occupy the middles of the links, or the classical and quantum spins alternate at the vertices of the lattice. The structures are shown schematically in figures 1(a) to 1(d).

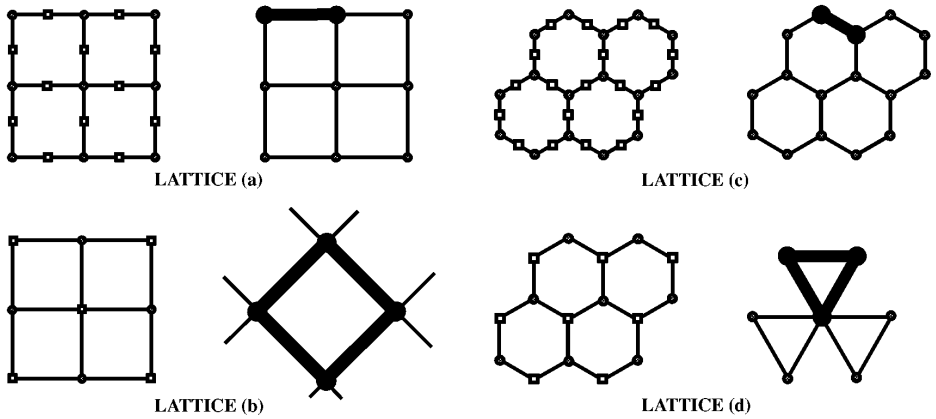

Figure 1. On the left-hand side of (a)–(d): the original lattices, where the squares stand for quantum spins, and the circles for classical spins. On the right-hand side of (a)–(d): the effective lattice of *classical* spins, with the unit cell bold.

In all cases, a quantum spin is surrounded only by classical ones. Therefore, the partition function can be factorized with respect to the quantum spin operators:

$$Z(T,H)=\int\left(\prod_{j=1}^{N_C}\mathrm{d}\Omega_j\right)\mathrm{Tr}_\sigma\left\{\prod_{i=1}^{N_Q}\exp\left(\boldsymbol{\sigma}_i\cdot\left[-\frac{1}{2}\beta JS\sum_{j\in V(i)}\boldsymbol{s}_j+\frac{1}{2}\beta g_2\mu_B H\hat{\boldsymbol{e}}_z\right]\right)\right\}$$
$$\times\ \exp\left(\beta g_1\mu_B SH\sum_{j=1}^{N_C}s_j^z\right).$$

In this expression, $V(i)$ is the set of labels of the classical spins that are the nearest neighbours of the quantum spin at site i. Let us call this set of classical spins a *unit cell*. Depending on the lattice, the unit cell is a link (lattices (a) and (c) of figure 1), a triangular plaquette (lattice (d)), or a square plaquette (lattice (b)). Due to the factorized form of $Z(T,H)$, the quantum spin dependence can be traced out to give a fully classical partition function:

$$Z(T,H)=\int\left(\prod_{j=1}^{N_c}\mathrm{d}\Omega_j\right)\left\{\prod_{\{\Gamma\}}2\cosh\left|\left|-\frac{1}{2}\beta JS\sum_{j\in\Gamma}\boldsymbol{s}_j+\frac{1}{2}\beta g_2\mu_B H\hat{\boldsymbol{e}}_z\right|\right|\right\}$$
$$\times\ \exp\left(\beta g_1\mu_B SH\sum_{j=1}^{N_c}s_j^z\right)\tag{1}$$

where $\{\Gamma\}$ is the set of unit cells on the lattice and $||\boldsymbol{X}||$ stands for the length of vector $\boldsymbol{X}$.

The original mixed-spin system is then equivalent to a classical one with an effective ferromagnetic interaction between the classical spins on the plaquettes $\{\Gamma\}$ which becomes (in zero field)

$$\mathcal{H}_{\mathrm{eff}}=-k_BT\sum_{\{\Gamma\}}\ln\left(2\cosh\left|\left|K\sum_{j\in\Gamma}\boldsymbol{s}_j\right|\right|\right).$$

In the following, we shall use the notation

$$K=\frac{1}{2}\frac{JS}{k_BT}\qquad\boldsymbol{W}(\Gamma)=\sum_{j\in\Gamma}\boldsymbol{s}_j\qquad W(\Gamma)=||\boldsymbol{W}(\Gamma)||\qquad W_z(\Gamma)=\boldsymbol{W}(\Gamma)\cdot\hat{\boldsymbol{e}}_z.$$

The various observables, like the heat capacity

$$C_V = k_B\beta^2 \frac{\partial^2}{\partial\beta^2} \ln Z(T,0)$$

and the zero-field susceptibility

$$\chi = \frac{k_B T}{V} \frac{\partial^2}{\partial H^2} \ln Z\bigg|_{H=0}$$

are simple generalizations of the ones defined in reference [12], and can be expressed as ensemble averages with respect to the Boltzmann weight $\mathrm{e}^{-\beta\mathcal{H}_{\mathrm{eff}}}/Z(T,0)$. By defining

$$E = -\frac{1}{2} JS \sum_{\{\Gamma\}} W(\Gamma) \tanh(KW(\Gamma))$$

we find that the internal energy and the specific heat are given by

$$U = \langle E\rangle_{\mathcal{H}_{\mathrm{eff}}}$$

$$C_V = k_B\beta^2[\langle E^2\rangle_{\mathcal{H}_{\mathrm{eff}}} - \langle E\rangle^2_{\mathcal{H}_{\mathrm{eff}}}] + k_B\langle\Phi\rangle_{\mathcal{H}_{\mathrm{eff}}} \qquad \text{with } \Phi = \sum_{\{\Gamma\}}\left[\frac{KW(\Gamma)}{\cosh(KW(\Gamma))}\right]^2. \tag{2}$$

The molar magnetic susceptibility is obtained from equation (1):

$$\chi = \frac{\mu_B^2}{k_B T N_M}\left(g_1^2 S^2\langle P\rangle_{\mathcal{H}_{\mathrm{eff}}} + Sg_1g_2\langle Q\rangle_{\mathcal{H}_{\mathrm{eff}}} + \frac{1}{4}g_2^2\langle R\rangle_{\mathcal{H}_{\mathrm{eff}}}\right) \tag{3}$$

where N_M is the number of molecules, and P, Q, and R have the following expressions†:

$$P = \left(\sum_{i=1}^{N_C} s_i^z\right)^2$$

$$Q = \left(\sum_{i=1}^{N_C} s_i^z\right)\left(\sum_{\{\Gamma\}} \bar{s}_z(\Gamma)\right)$$

$$R = \left(\sum_{\{\Gamma\}} \bar{s}_z(\Gamma)\right)^2 - \sum_{\{\Gamma\}} (\bar{s}_z(\Gamma))^2 + \sum_{\{\Gamma\}}\left((1-\rho^2(\Gamma))\frac{\tanh(KW(\Gamma))}{KW(\Gamma)} + \rho^2(\Gamma)\right)$$

where $\rho(\Gamma) = W_z(\Gamma)/W(\Gamma)$ and $\bar{s}_z(\Gamma) = -\rho(\Gamma)\tanh(KW(\Gamma))$.

3. Monte Carlo simulations

These various thermodynamical quantities are determined by Monte Carlo sampling, with respect to the Boltzmann weight $\mathrm{e}^{-\beta\mathcal{H}_{\mathrm{eff}}}/Z(T,0)$. The simulations were first performed using the Metropolis method [17]. This method has been proved to be very useful at high temperature, far from the phase transition. However, it suffers from a severe slowing down near the phase transition, and therefore becomes rather inefficient at low temperature, since, for an isotropic two-dimensional system, the critical temperature is $T_C = 0$ K [18]. A cluster-flipping method developed by Wolff [19] drastically reduces the slowing down, and the Wolff algorithm was used for high values of K (i.e. low values of T). To overcome the finite-size effects in the critical region, we increased the size of the systems as T decreased. The number of cells was 2^{14} for $K < 2$, and increased up to 2^{16} for $K = 5$. Periodic

† The numerical values of $\langle P\rangle_{\mathcal{H}_{\mathrm{eff}}}$, $\langle Q\rangle_{\mathcal{H}_{\mathrm{eff}}}$, and $\langle R\rangle_{\mathcal{H}_{\mathrm{eff}}}$ as functions of the temperature for the four lattices can be provided on request.

boundary conditions were imposed on the system, and a random spin configuration was taken as the initial spin configuration. The number of Metropolis steps necessary to reach the thermal equilibrium was found to be between 10^2 and 10^4 lattice sweeps depending on the temperature. The averaging of the various observables was stopped when $\Delta\chi/\chi < 0.01$. The relative uncertainty in the energy and the specific heat was then better than 10^{-2}. These calculations were performed on a Cray J916.

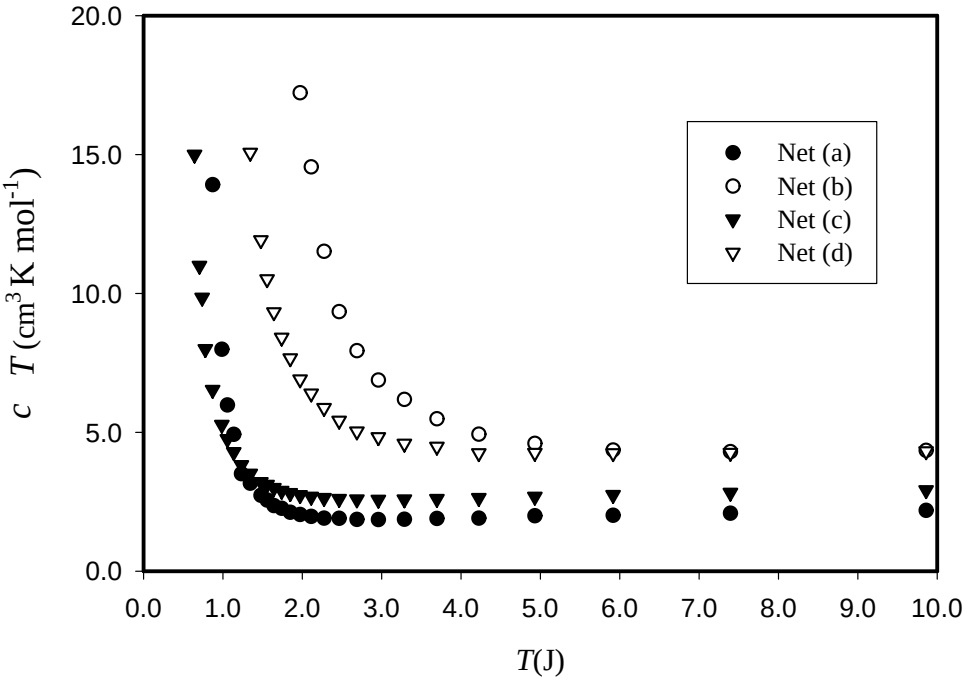

Figure 2. χT (in units of cm^3 K mol^{-1}) as a function of temperature (in units of J). The local spins are assumed to be $S_C = S(\mathrm{Mn}) = 5/2$ and $S_Q = S(\mathrm{Cu}) = 1/2$, and the local Zeeman factors are taken to be $g_1 = g_2 = 2$. The labels refer to the lattices of figure 1.

3.1. The magnetic susceptibility

Figure 2 shows the behaviour of χT (in cm^3 K mol^{-1}) as a function of the temperature (in units of J) for the four lattice configurations. The four curves present the same general trend, characterized by the following features:

(i) a constant value at high temperature corresponding to the paramagnetic limit;

(ii) a shallow minimum, characteristic of a ferrimagnetic system with antiferromagnetic couplings; this is due to the local ordering appearing as the temperature is lowered, and which causes a decrease of the local magnetization;

(iii) a rapid increase at low temperature due to the critical divergence at $T = 0$.

It is interesting to determine the extent to which all of these results can be described by the same universal trend, simply corrected by the lattice effects. In fact, at high temperature, the susceptibility is given by the Curie constant, which depends in a simple way on the spin

arrangement:

$$(\chi T)_{T=\infty} = \frac{\mu_B^2}{3k_B}\left[\frac{35}{4}n_C g_1^2 + \frac{3}{4}n_Q g_2^2\right] \tag{4}$$

where n_Q and n_C are the numbers of low-spin (quantum) and high-spin (classical) ions per molecule, respectively (these numbers are given in table 1 for each lattice). In equation (4) we have taken $S^{(Q)} = 1/2$, $S^{(C)} = S(\mathrm{Mn}) = 5/2$. For the curves of figure 2 we set $g_1 = g_2 = 2$.

Table 1. n_Q (n_C) is the number of quantum (classical) spins per molecule. T_m^χ is the temperature (in units of J) at which the minimum of χT occurs: (MC) (column 4) from the Monte Carlo data, and (MF) (column 5) from the mean-field theory. $\tilde{J}$ is the effective coupling of the non-linear sigma model deduced from the low-temperature limit of the lattice model.

Network	n_Q	n_C	T_m^χ (MC)	T_m^χ (MF)	$\tilde{J}$
(a)	2	1	3 ± 0.5	5.83	$\frac{1}{4}JS$
(b)	$\frac{1}{2}$	$\frac{1}{2}$	7.4 ± 1	11.7	$\frac{1}{2}JS$
(c)	3	2	3 ± 0.1	5.83	$JS/4\sqrt{3}$
(d)	1	1	6 ± 1	8.78	$JS/2\sqrt{3}$

The temperature at which the minimum occurs is determined from the Monte Carlo data. We present the results in table 1 (column 4) for each lattice. We have computed this quantity within the mean-field theory, and we found the surprisingly simple result

$$T_m^\chi(\mathrm{MF}) = \frac{1}{3}JS^2n$$

where n is the number of classical spins in a unit cell (or equivalently the number of classical neighbours of a quantum spin). These values are presented in the fifth column of table 1. Although the mean-field and Monte Carlo results are quantitatively different, one can see from table 1 that the relative positions of the minima with respect to the lattice are the same for the two results. This is an indication that the parameter n is probably relevant to this quantity.

At low temperature, the critical divergence is described by the non-linear sigma model. The mapping between the discrete model on a specific lattice and the universal field theory can be established as follows. First, take the low-temperature spin-wave limit of the lattice model:

$$\mathcal{H}_{\mathrm{eff}}(J) \longrightarrow \mathcal{H}_{\mathrm{SW}}(J^*) = -\frac{1}{2}J^*\sum_{\langle ij\rangle}\theta_{ij}^2.$$

Then take the long-wavelength limit in order to go to the continuum model:

$$\mathcal{H}_{\mathrm{SW}}(J^*) \longrightarrow \mathcal{H}_\sigma(\tilde{J}) = \frac{1}{2}\tilde{J}\int \mathrm{d}^2r \ \sum_\mu \partial_\mu \boldsymbol{n}(\boldsymbol{r})\cdot\partial_\mu\boldsymbol{n}(\boldsymbol{r}). \tag{5}$$

The first step depends on the effective interaction between the classical spins whereas the second is related to the geometry of the classical spin lattice. The expression for $\tilde{J}$ is given in table 1 for each lattice model. As a consequence, we expect a universal behaviour of the low-temperature regime for all of the lattices, provided that the temperature is renormalized in such a way that $\tilde{T} = T/\tilde{J}$. We do not observe this behaviour *quantitatively* in our Monte

Carlo data, since our lowest temperatures do not lie within the universal critical regime†. However, the hierarchy of the $\tilde{J}$-values gives the relative positions of the critical increases of χT for each lattice fairly well qualitatively.

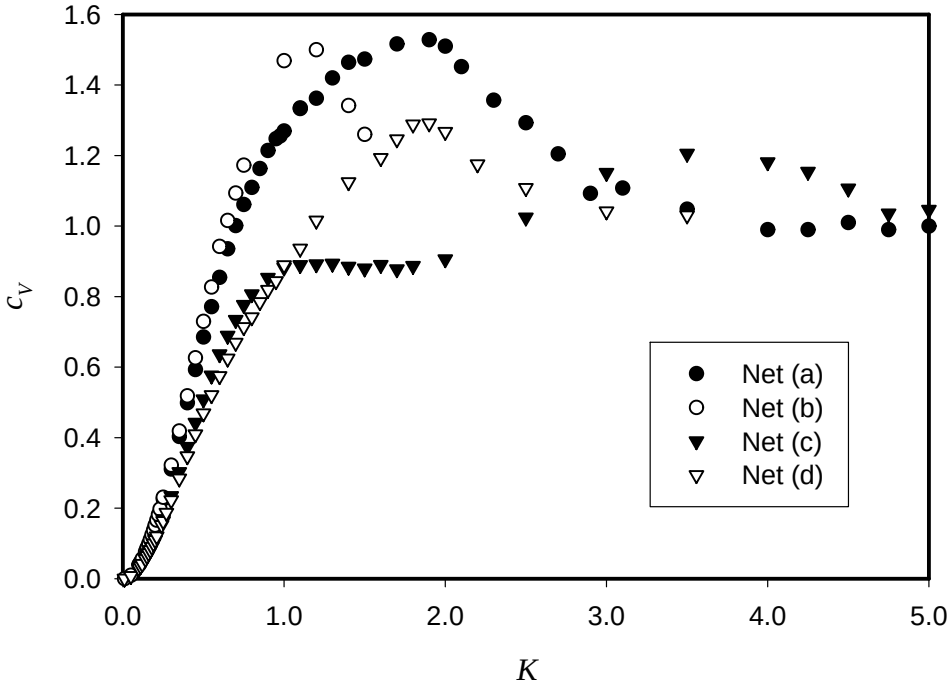

Figure 3. The specific heat $c_V = C_V/(N_C k_B)$ versus $K = JS/(2k_B T)$ for the four lattices.

Table 2. Coefficients of the high-temperature expansion for c_V for the four lattices.

Lattice	a_2	a_4	a_6
(a)	4	$-\frac{20}{3}$	8
(b)	4	-4	$-\frac{152}{9}$
(c)	3	-5	6
(d)	3	-7	$\frac{140}{9}$

3.2. The specific heat

The specific heat is plotted as a function of K in figure 3 for the four types of lattice. In all cases, it presents a well pronounced maximum. In addition to this common trend, the dependence on the lattice geometry of the details of these curves can be understood from simple arguments. The $T = 0$ (large-K) limiting value can be obtained from the spin-wave contribution to the Hamiltonian of equation (5), which gives an energy *per classical spin* of

$$E \approx E_0 + k_B T.$$

† We noticed in reference [12] that this behaviour is observed for lattice (c) for $K \gtrsim 2.5$ which corresponds to $T \lesssim 0.59J$.

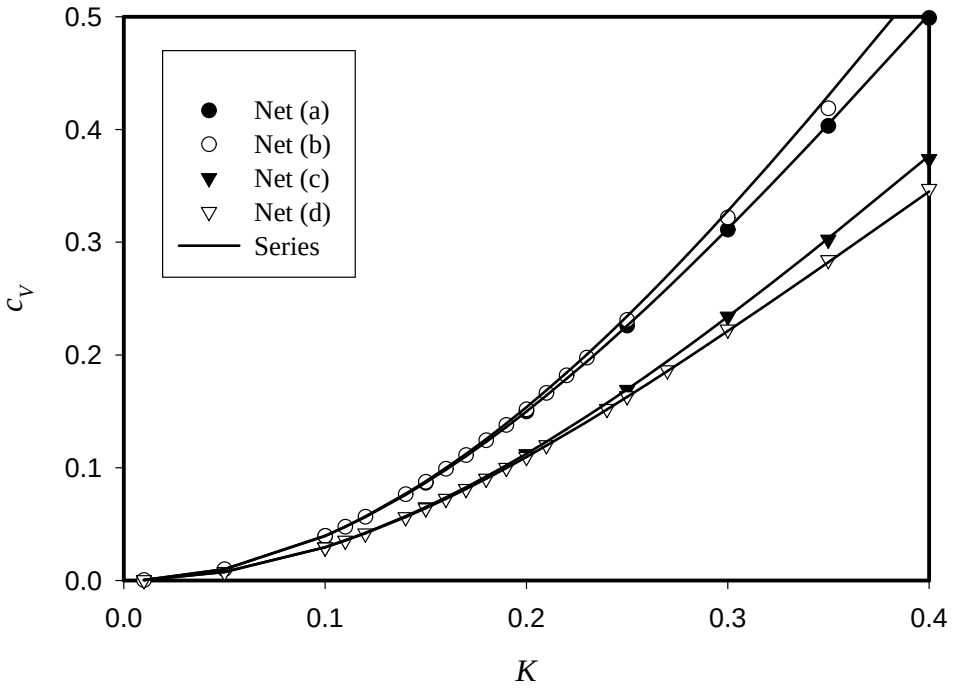

Figure 4. As figure 3, but in the high-temperature regime. The data points correspond to the Monte Carlo results and the lines to the low-order high-temperature expansion.

Therefore, by normalizing the heat capacity with respect to the number of classical spins, we get, for $T = 0$, $c_V = C_V/N_C k_B = 1$ as can be seen in figure 3 from the result of the simulation†. For large T (small K), the behaviour of the specific heat can be inferred from the high-temperature expansion. The first few terms of this expansion can be derived easily, and we get

$$c_V = a_2 K^2 + a_4 K^4 + a_6 K^6 + \cdots$$

where a_2 turns out to be the number of unit cells connected to a single (classical) site. This number and the coefficients a_4 and a_6 are given in table 2 for each lattice. The result, presented in figure 4 in comparison with the Monte Carlo data, shows that, up to $K \simeq 0.4$, the system is driven by its high-temperature behaviour.

The behaviour at intermediate and low temperature depends on the superposition of two contributions, similarly to the case of lattice (c) already analysed in reference [12], where this effect is clearly visible.

(i) A bump for $K \approx 1$–2 resulting from the local ordering of the quantum spins with respect to their randomly distributed classical neighbours. By neglecting the correlations between the classical spins, we can estimate this contribution

$$C_V^Q \simeq N_Q k_B K^2 \int \prod_{i\in\Gamma} \frac{\mathrm{d}\Omega_i}{4\pi} \; \frac{W^2(\Gamma)}{\cosh^2(KW(\Gamma))}. \tag{6}$$

† A non-zero value of the specific heat at zero temperature reminds us of the approximation of 5/2 quantum spins by classical spins.

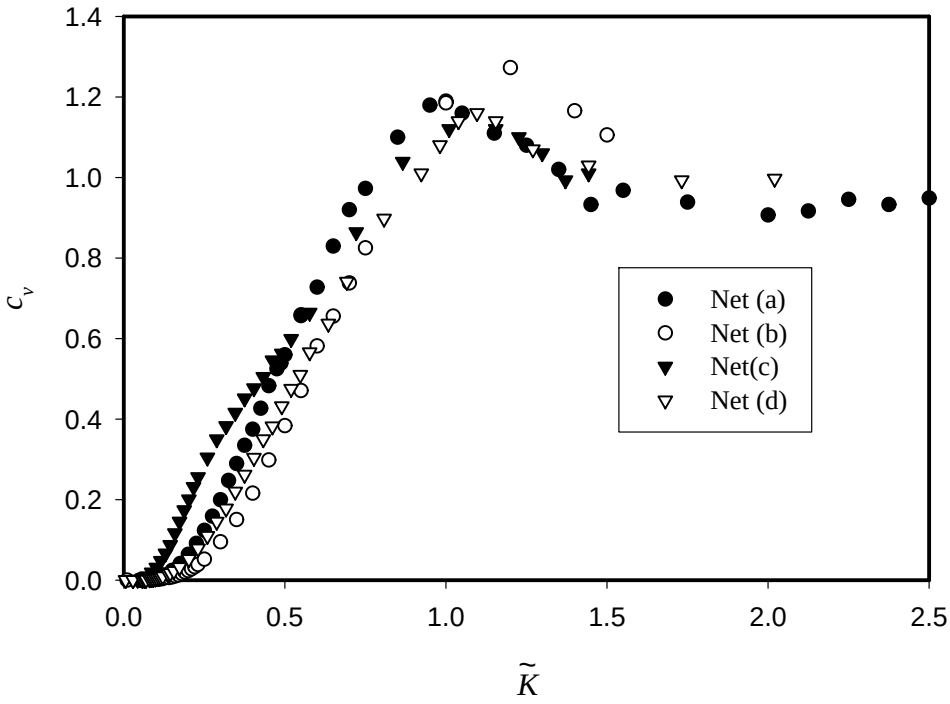

Figure 5. The specific heat subtracted from the quantum spin contribution as a function of the lattice-renormalized coupling $\tilde{K} = \tilde{J}/JK$ (see table 1).

(ii) A low-temperature behaviour, described by the universal limit of the model (equation (5)), provided that the temperature is renormalized by the factor defined in the preceding section.

Accordingly, by subtracting the specific quantum contribution given by equation (6) and renormalizing the temperature dependence of the residual specific heat, we expect to single out a typical curve, free of geometrical effects. This is what we can observe in figure 5, where the dependence of the lattice has been washed out by comparison with figure 3. The bump seen on this curve is already present in the specific heat of the standard 2D classical Heisenberg model, but we have no convincing explanation of its origin. It would be interesting to obtain experimental confirmation of this effect.

4. Conclusion

In this paper we have determined the effect of the topology of the spin lattice on the thermodynamical properties of two-dimensional systems with alternating quantum–classical spins, modelling a wide family of magnetic molecular compounds. Since the quantum spin dependence can be traced out, we can use the very powerful *classical* Monte Carlo techniques to analyse these systems.

We found that the temperature dependences of both the magnetic susceptibility and the specific heat can be described on the grounds of general behaviours in which the lattice influence is explicit. Thus we are able to obtain a typical function for the specific heat, which is independent of the lattice geometry. This analysis allows one to predict, in principle, what

the specific heat and the magnetic susceptibility would be for other compounds with different spin geometries. Alternatively, it can be used to determine the interaction parameters together with the Zeeman factors from experimental data [10].

In most cases [3], one observes experimentally at low temperature (typically 10 to 15 K) a transition towards a ferromagnetic ordered phase which cannot be accommodated within our isotropic interaction [18]. Therefore, the present analysis is only valid in the paramagnetic phase. At low temperature, spin anisotropy [11] and/or spatial anisotropy must be taken into account to explain this ferromagnetic phase transition.

References

[1] Kahn O 1993 *Molecular Magnetism* (New York: VCH)
[2] Gatteschi D, Kahn O, Miller J S and Palacio F 1991 *Magnetic Molecular Materials (NATO ASI Series E, vol 198)* (Dordrecht: Kluwer)
[3] Mathonière C, Kahn O, Daran J C, Hilbig H and Köble F H 1993 *Inorg. Chem.* **32** 4057
[4] Seiden J 1983 *J. Physique Lett.* **44** L947
[5] Drillon M, Gianduzzo J C and Georges R 1983 *Phys. Lett.* **96A** 413
[6] Verdaguer M, Gleizes A, Renard J P and Seiden J 1986 *Phys. Rev.* B **29** 5144
[7] Georges R, Curély J, Gianduzzo J C, Xu Q, Kahn O and Pei Yu 1988 *Physica* B+C **77** 153
[8] Drillon M, Coronado E, Georges R, Gianduzzo J C and Curély J 1989 *Phys. Rev.* B **40** 10 992
[9] Stumpf H O, Pei Yu, Kahn O, Sletten J and Renard J P 1993 *J. Am. Chem. Soc.* **115** 6738
[10] Larionova J, Mombelli B, Sanchiz J and Kahn O 1998 *Inorg. Chem.* at press
[11] Meyers C, Meurdesoif Y, Leroyer Y and Kahn O 1998 *J. Phys. C: Solid State Phys.* **10** 2065
[12] Leandri J, Leroyer Y, Meshkov S V, Meurdesoif Y, Kahn O, Mombelli B and Price D 1996 *J. Phys. C: Solid State Phys.* **8** L271
[13] Tamaki H, Zhong Z, Matsumoto N, Kida S, Koikawa M, Achiwa N, Hashimito Y and Okawa H 1992 *J. Am. Chem. Soc.* **114** 6974
[14] Atovmyan L O, Shilov G V, Lyubovskaya R N, Zhilyaeva E I, Ovanesyan N S, Pirumova S I, Gusakovskaya I G and Morozov Y G 1993 *JETP Lett.* **58** 766
[15] Decurtins S, Schmalle H W, Schneuwli P and Oswald H R 1993 *Inorg. Chem.* **32** 1888
[16] Decurtins S, Schmalle H W, Oswald H R, Linden A, Ensling J, Gütlich P and Hauser A 1994 *Inorg. Chem. Acta* **216** 65
[17] Metropolis N, Rosenbluth A W, Rosenbluth M N, Teller A H and Teller E 1953 *J. Chem. Phys.* **21** 1087
For a review, see
Landau D P 1992 *Monte Carlo Simulations in Condensed Matter Physics* ed K Binder (Heidelberg: Springer) and references therein
[18] Mermin N D and Wagner H 1966 *Phys. Rev. Lett.* **17** 1133
[19] Wolff U 1989 *Phys. Rev. Lett.* **62** 361